J. Agr. Sci. Tech. (2009) Vol. 11: 549-558

MODIS NDVI Quality Enhancement Using ASTER Images

E. Javadnia[1], M. R. Mobasheri[1*], and Gh. A. Kamali[2]

ABSTRACT

Sensors onboard meteorological satellites such as MODIS and AVHRR are able to collect information adequate in frequency but with low spatial resolution. The problem can be overcome, if one finds a way to increase the quality of the vegetation indices through searching in each individual pixel of the images, employing concurrent higher spatial resolution images. The objective of this study was to investigate the enhancement of MODIS NDVI products by using NDVI from the ASTER sensor onboard the same platform, as MODIS. The ASTER averaged NDVI values computed using only vegetated pixels were compared to unadjusted MODIS NDVI. Two approaches for the comparison are introduced in this work. In the first one, vegetated ASTER NDVI compared with MODIS NDVI (AMII Model), and in the second one the difference between vegetated ASTER NDVI and MODIS NDVI was modeled against a code representing percentage of vegetation cover (AMDI Model). It is found that the MODIS NDVI index always reads lower as compared to the vegetated ASTER NDVI. It was also found that the difference between vegetated ASTER NDVI and MODIS NDVI for vegetation covers of less than 20% was greater than 0.1 and for vegetation covers of more than 80% as low as 0.01. This could produce erroneous results when introducing uncorrected NDVI values into the climatological models especially in the arid and semi-arid climates where the vegetation covers are sparse. Both AMII and AMDI models produce NDVI values higher than those calculated from MODIS. These models were tested using 10 samples where a RMSE of about 0.028 for AMII and 0.018 for AMDI was found out. It is revealed that AMII model increases the NDVI values up to 87% for pixels containing less than 10% vegetation while 5% for pixels with more than 80% vegetation covers. These increases for AMDI model were 84% and 6%, respectively.

Keywords: Image Processing, Remote Sensing, Vegetation.

INTRODUCTION

The use of satellite remote sensing in monitoring changes in biospheric processes such as vegetation cover, phenology, primary production, crop yield, evapotranspiration, and many other physiological and climatological parameters requires frequent repeated observations (Sellers and Schimel, 1993; Townshend *et al.,* 1994; Mobasheri *et al.,* 2008).

While fluctuations in annual precipitation plays a vital role in land productivity in such arid and semi-arid regions as Iran, long-term changes in vegetation condition is likely to be the result of other natural and anthropogenic factors. Physical features of geomorphology and soils, in addition to human actions like changing land use practices, urban expansion, overgrazing, and protected resource areas all contribute to the productivity of land in a given region. One of the main parameters for developing any drought model is the definition of an index describing the vegetation covers in the region (Reed *et al.,* 1994).

Thiam (2003) in his recent study used these data to analyze the causes of spatial

[1] Remote Sensing Engineering Department, Khajeh Nasir Toosi University of Technology, Tehran, Islamic Republic of Iran.
[2] Iran Meteorological Organization, Tehran, Islamic Republic of Iran.
[*] Corresponding author, e-mail: mobasheri@kntu.ac.ir

[DOR: 20.1001.1.16807073.2009.11.5.7.4]

patterns of land degradation in a region in the west of Africa. He used 1 km Normalized Difference Vegetation Index (NDVI) in conjunction with other measures of socio-economics, rainfall, soils, as well as aerosols to assess land degradation risk in southern Mauritania. These data provided a measure of primary biomass production that was employed to identify areas at risk of degradation. Thiam identified overgrazing and erratic rainfall patterns as a major cause of land degradation.

Natural factors affecting vegetation productivity include precipitation variability, wind and water erosion and many more. Of these, precipitation is the primary limiting factor on both cropland and natural vegetation systems. The semi-arid regions of the country have experienced periodic drought and declining rainfall throughout the twentieth century.

Large-area studies of the region have characterized the relationship between rainfall and vegetation productivity using NDVI (Malo and Nicholson, 1990; Milich and Weiss, 2000; Li *et al.,* 2004).

NDVI is well established in the literature as being a good representation of vegetation growth and phenology (Reed *et al*., 1994; Jiang *et al*., 2006). NDVI is calculated from surface reflectance in the near-infrared ρ_{NIR} and red ρ_R portions of the electromagnetic spectrum, using the following formula:

$$NDVI = \frac{\rho_{NIR} - \rho_R}{\rho_{NIR} + \rho_R} \quad (1)$$

NDVI index varies between -1 and 1 where its values for vegetated land are generally greater than 0.2, with values exceeding 0.5 indicating dense vegetation.

Many research works in the field of climatology have focused on using extended time-series of NDVI derived from the satellite images. Sensors such as Advanced Very High Resolution Radiometer (AVHRR) have provided Global Area Coverage of NDVI from 1982 to the present at a spatial resolution of 4 km where these data are distributed globally at a degraded resolution of 8 km.

Although it provides an extensive temporal record for comparison, the coarse spatial resolution of these data limits their effectiveness at detecting local scale variability, which is of concern for local to regional planning.

The development of drought prediction models depends on an unambiguous, replicable definition of the existing terrestrial vegetation. Vegetation characteristics such as amount of coverage and phenology affect processes such as water cycling, absorption and reemission of solar radiation, momentum transfer, carbon cycling, as well as latent and sensible heat fluxes. Consequently, variations in the composition and distribution of vegetation represent one of the main sources of systematic land cover changes on local, regional, or global scale, and the ability to precisely detect these variations, using multi-temporal remotely sensed image data is of utmost importance for both environmental research projects and management activities (Hall *et al.*, 1995; Jiang *et al.,* 2006). This problem is even more dramatic when dealing with areas where desertification processes may occur (Bolle, 1996).

The only two currently operating remote sensing platforms which are capable of providing the temporal frequency necessary for monitoring such processes are the AVHRR instrument onboard the NOAA series of meteorological satellites and the Moderate-resolution Imaging Spectroradiometer (MODIS) onboard the Terra and Aqua platforms. Unfortunately, these two sensors may be at a coarser spatial resolution than some applications require. Thus it is important to be able to utilize techniques that enhance data acquired from these sensors, allowing them to be used more effectively.

The images so far used for this purpose have usually been low of spatial resolutions. This means that each individual pixel may contain different features with different

[DOR: 20.1001.1.16807073.2009.11.5.7.4]

spectral characteristics. This may in turn decrease the applicability of the calculated indices and consequently render the useful application of drought models prohibitive. On the other hand, sensors onboard of meteorological satellites such as the MODIS and AVHRR are able to collect information frequently enough but with low spatial resolution. This spatial resolution problem can be overcome, if one finds a way to estimate the actual vegetation response from within each pixel. This will be done by linearly transforming the NDVI values as a function of pixel-level vegetation fraction estimates, which are estimated using higher resolution imagery.

The objectives of this study were to extend these analyses to an investigation of the improvement of the capability of MODIS NDVI products by using data from the ASTER sensor onboard the same platform as MODIS. This may increase the accuracy of NDVI, and other vegetation indices derived from a number of multi-temporal, multi-resolution satellite sensors through several growing seasons and kept in archives around the world.

Based on remote sensing data, the existence of sources of errors and uncertainties in input data can reduce the applicability of many climatological models. One of these models is drought prediction model in which satellite images with proper spatial and temporal resolution and, to some extent, proper spectral resolution are needed. These three factors cannot concurrently be found in any of the available remote sensing products. Some remote sensing products such as MODIS have suitable temporal and spectral resolution but are poor in spatial. Each pixel of MODIS NDVI contains an area of about 6.5 hectares in the best viewing conditions. For such arid and semi-arid regions as Iran, vegetation cover is sparse and this means that the pixels are a mixture of different surface covers and the calculated NDVI is not necessarily the reflection of the vegetation present in the pixel. This uncertainty may be reduced if one can estimate the vegetation cover fraction within each MODIS pixel using higher resolution ASTER data, and then use this information to transform MODIS NDVI values to represent only the vegetated portion of the pixel. This is the would be objective of this work.

Site Selection and Data

The region of study is a part of Amirkabir and Dea`bal-Khazaie Sugarcane Sites located at the north of Ahwaz between 31°14'7"N–31°54'20"N latitude and 48°21'52"E–49°14'56"E longitude, some 20 m height from sea level. The location of the field in the UTM system is in zone 39, from 237361m to 239506m in length and from 3427183m to 3428158m in width (Figure 1). The reason for this selection was the collection of field data on a routine basis in the above-mentioned sites. The climate is hot and dry with temperature varying between -7°C in winter to +54°C in summer.

The annual precipitation is 231 mm with an average evaporation of 9,300 mm per annum (Mobasheri *et al.,* 2007). The deficiency is compensated for through irrigation using water from the two rivers of Karoon and Bahmanshir.

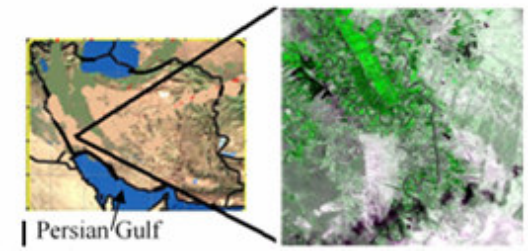

Figure 1. Study area located at the north-west of Persian Gulf.

Ahwaz is the largest city in Khuzestan Province. This city along with its districts with 386,405 hectares of agricultural fields is one of the agricultural poles in the region (Mobasheri *et al.,* 2007). The selected field is a part of Amirkabir Sugarcane Unit, a part of 84,000 hectares of sugarcane industries.

Following a screening of 10 MODIS and ASTER images for weather conditions,

[DOR: 20.1001.1.16807073.2009.11.5.7.4]

dustiness, as well as availability of field data, two MODIS and two ASTER images acquired on November 8, 2004 and August 12, 2004 were selected as study tools to be used in theresearch. Each of the Level1-B Terra/ASTER images in bands 2 and 3N were a part of MODIS scene acquired on the same time containing different surface covers including sugarcane in different proportions. To ensure the quality of satellite images, analysis of the weather condition was carried out. Moreover, subsets of satellite images for different parts of MODIS scene were produced. Satellite images were corrected for Khuzestan atmosphere, using weather data and orbital parameters, although we only compare ASTER and MODIS of the same scene where the relative correction of the atmosphere may suffice. Also geometrical correction was made by rotating the ASTER image by an angle given in the image header. Maps of 1:25000 were employed in the image geo-referencing control process. This correction for MODIS was done by Iran Space Agency.

Two bands of red and near-infrared in ASTER and MODIS were used in the research (Table 1). ASTER Bands 3N (NIR) and 2 (Red) and MODIS bands 1 and 2 were then converted into apparent reflectance values. Since it was intended to compare ASTER and MODIS images of the same scene, neither atmospheric nor topographic corrections were performed at this stage. Using apparent reflectance images in Red and NIR bands, the NDVI index was computed using equation (1) for ASTER images.

Table 1. ASTER and MODIS bands used in this work.

	Band no.	Spatial resolution (m)	Band width (μm)
ASTER	2	15	0.63-0.69
	3N	15	0.78-0.86
MODIS	1	250	0.62-0.67
	2	250	0.841-0.876

The level 2 MODIS data were supplied from Iranian Space Agency's archive on the same day that ASTER images were acquired. A sub-scene of 80×73 pixels was extracted from each of the two ASTER images and the image-to-image registration procedure was done. Also a nearest-neighbor resampling algorithm was applied that was trained for 4 ground control points selected in the ASTER image, with a final RMSE lower than 1 pixel on both axes. Projection UTM WGS 84 north zone 39 was applied for both MODIS and ASTER images. MODIS Band 2 (NIR) and Band 1 (R) were then converted into apparent reflectance values. Using these two apparent reflectance images, the NDVI index image was computed using (1).

METHODOLOGY

To compare MODIS image with ASTER, the following steps were taken:

Step 1: Selecting one arbitrary MODIS pixel in the NDVI image with spatial resolution of 250m (Figure 2).

Step 2: Overlaying ASTER NDVI image of the same date on the MODIS NDVI image. Each MODIS pixel contains approximately 17 by 17 ASTER pixels (Figure 3).

Step 3: The simplest way to separate pixels containing full or partial vegetation cover from nonvegetated pixels is by imposing some threshold value for NDVI. This threshold value is selected to be 0.2 (Hall and Sellers, 1995). This threshold was imposed on each 17 by 17 ASTER pixels (equivalent to one MODIS pixel) to classify the vegetated pixels (Figure 4). Then the averaged NDVI values of the vegetated pixels were calculated.

Step 4: 45 samples were selected from the MODIS NDVI image. These samples included pixels of different vegetation cover fractions (different values of NDVI all greater than 0.2).

[DOR: 20.1001.1.16807073.2009.11.5.7.4]

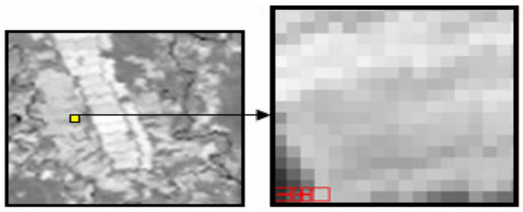

Figure 2. A MODIS NDVI image (left) and an ASTER NDVI image overlaying a MODIS pixel (right).

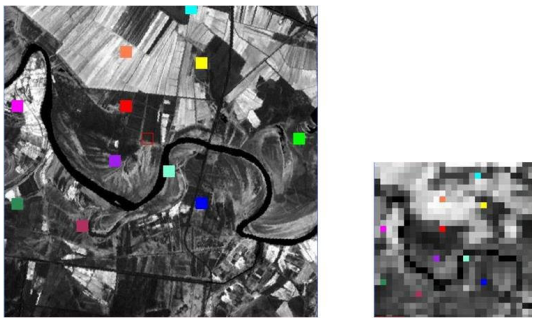

Figure 3. A portion of MODIS NDVI (right) and ASTER NDVI image (left). A part of Karoon River can be seen in the image (images are not of the same scale). Boxes on both images are selected samples.

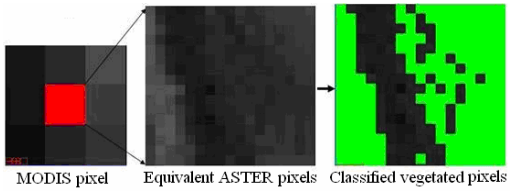

Figure 4. Procedure of classification of vegetated ASTER pixels (green). Each 17 by 17 ASTER NDVI pixel corresponds to one underlying MODIS pixel.

By using land use maps prepared by Sugarcane Industry, pixels of the same kind of vegetation cover (namely sugarcane) are selected. This will limit the effects of spectral signatures in the mixed pixels.

Vegetated ASTER NDVI values were compared with the corresponding MODIS NDVI values and a regression analysis of these values carried out (Alesheikh and Sadeghi, 2007). Figure 5 shows a plot of NDVI values extracted from MODIS (triangles) and averaged over corresponding vegetated ASTER pixels. The values are sorted out according to percentage of vegetation covers. The purpose of the regression modeling is to close the gap between MODIS and ASTER NDVI using an appropriate transformation of the MODIS NDVI values as a function of vegetation cover fraction. The resulting transformed MODIS NDVI values are considered to be improved for use in climatological models, because they better represent NDVI from just the vegetation within each MODIS pixel.

The analysis of the results shows improvements for the MODIS NDVI values particularly for low vegetated pixels. This will be discussed in the following sections. The above 4 steps can be summarized in a conceptual flowchart shown in Figure 6.

As expected, the two values of NDVI follow each other and appear to increase converge as NDVI increases. As shown in Figure 5, vegetated ASTER NDVI reads almost twice that of the MODIS in sparse vegetation pixels (low NDVI).

Modeling

Taking into account the calculated NDVIs, two models can be suggested. In the first one, the linear relationship between ASTER NDVI (calculated from vegetated pixels) and MODIS NDVI was determined. For simplicity of referencing, this model will be called ASTER-MODIS Improved Index (AMII). In the second model, the difference of vegetated ASTER NDVI and MODIS NDVI was plotted against some codes representing the amount of vegetation proportion in the pixels. This model will be addressed by ASTER-MODIS Difference Index (AMDI).

As seen in Figure 5, MODIS NDVI always reads lower as compared to vegetated ASTER NDVI. This was due to the presence of mixed pixels with a low portion of vegetative cover. Since non-vegetated surfaces typically have lower NDVI values as compared to vegetation, the

[DOR: 20.1001.1.16807073.2009.11.5.7.4]

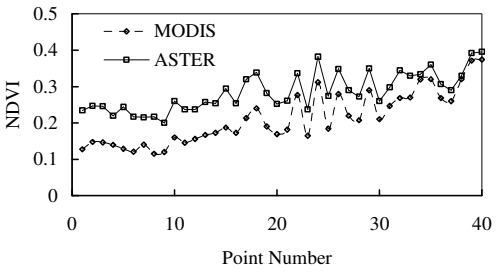

Figure 5. MODIS and vegetated ASTER NDVI from the same MODIS pixels.

mixed pixels have similar reflectance in both NIR and RED and consequently lower values of NDVI. These mixed pixels may sometimes be marked as bare soil or even water. It is found that the difference between ASTER NDVI and MODIS NDVI for vegetation covers of less than 20% was greater than 0.1, and for vegetation covers of more than 80% as low as 0.01. This could produce erroneous results when introducing uncorrected NDVI values into the climatological models, especially in arid and semi-arid climates where the vegetation covers are sparse.

AMII Model

To prepare the AMII model, 40 out of 45 samples were used. The other 5 pixels were suspected to be contaminated with the small patches of clouds that could not be detected through MODIS cloud masking algorithms but were detected through ASTER's. Then the vegetated ASTER NDVI values were drawn against MODIS NDVI values (Figure 7). A linear fit to these data by least square method produces an equation of the form:

$$NDVI_{MODIS}(Imp) = 0.6951 NDVI_{MODIS} + 0.1377 \quad (2)$$

Equation (2) has an R^2 of 0.906, and holds for $NDVI_{MODIS} \leq 0.45$. For any value of $NDVI_{MODIS}$ greater than 0.45, it is assumed that the pixels are fully vegetated and consequently no adjustment of MODIS NDVI is needed.

AMDI Model

AMDI model was created in two steps. In the first step a relationship between the Vegetation Fraction Cover (VFC) in each MODIS pixel and the pixel's NDVI was produced (Figure 8). The linear equation best describing this relationship is

$$VFC = 3.5972.NDVI_{MODIS} - 0.2976, \quad R^2 = 0.776 \quad (3)$$

Equation (3) holds for $NDVI_{MODIS} \leq 0.36$ and for $NDVI_{MODIS}$ greater than 0.36, while VFC taken to be 1. The effects of this

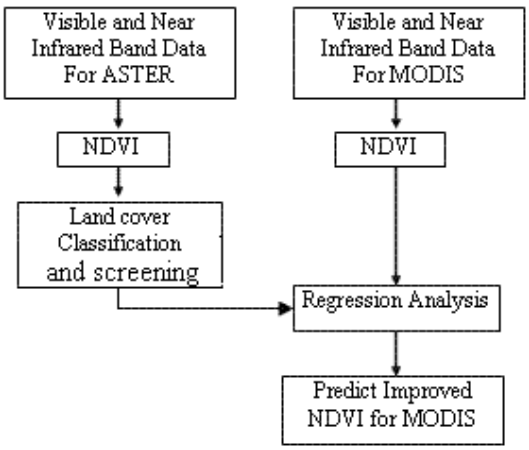

Figure 6. A conceptual flowchart of the research.

[DOR: 20.1001.1.16807073.2009.11.5.7.4]

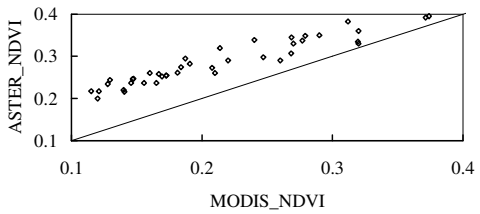

Figure7. Vegetated ASTER NDVI vs. MODIS NDVI (AMII Model).

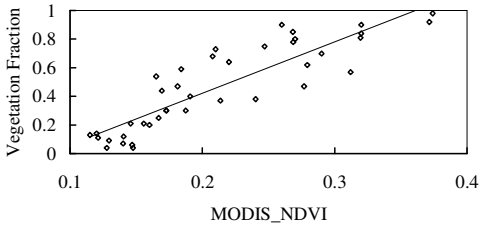

Figure 8. A plot of the fraction of vegetation vs. MODIS NDVI.

assumption will be discussed shortly. The calculated VFC values using (3) were grouped into 10 classes according to their percentage covers, assigning a code of 1 to 10 to each (Table 2).

This binning operation was adopted to accommodate the uncertainties involved with the calculation of NDVI due to the environmental parameters and atmospheric effects (Mobasheri *et al*., 2007; Mobasheri *et al.,* 2008). So instead of using an exact value of NDVI, a code will be assigned to it. This will create a bigger space for the errors involved with the remote sensing in this regard.

In the next step, using these codes, a regression between the differences of vegetated ASTER NDVI and MODIS NDVI (error values), and the codes was setup (Figure 9). A linear fit to these data had an equation of the form:

$$NDVI_{ASTER} - NDVI_{MODIS} = -0.0079.Code + 0.1148 \quad (4)$$

where the improved NDVI values can be calculated using the following equation:

$$NDVI_{MODIS}(Imp) = -0.0079.Code + 0.1148 + NDVI_{MODIS} \quad (5)$$

The distribution in the scatterplot of Figure 9 may look more curvilinear than linear but generally it is advisable to use a basic linear model in situations with many uncertainties. Of course, more advanced models could be introduced if more *in situ* data could be collected.

RESULTS AND DISCUSSION

An evaluation of the suggested models AMII and AMDI is the final concluding step in this work. For this the Root Mean Squared Error (RMSE) of the observed and predicted NDVI values calculated using the following equations:

$$\text{RMSE} = \sqrt{\frac{r_i^2}{n}} \quad \text{with}$$

$$r = NDVI_{obs} - NDVI_{pre} \quad , i = 1,2,...n$$

$NDVI_{obs}$ is the vegetated ASTER NDVI for the check points in the ASTER images and is taken as ground truth. $NDVI_{pre}$ is the NDVI calculated from either the AMII or AMDI model. Symbol *n* represents the number of check points. Ten samples have been used as check points for evaluation at this stage. These check points

Table 2. Codes for different fractions of vegetation covers.

Vegetation density (%)	0-10	10-20	20-30	30-40	40-50	50-60	60-70	70-80	80-90	90-100
Code	1	2	3	4	5	6	7	8	9	10

[DOR: 20.1001.1.16807073.2009.11.5.7.4]

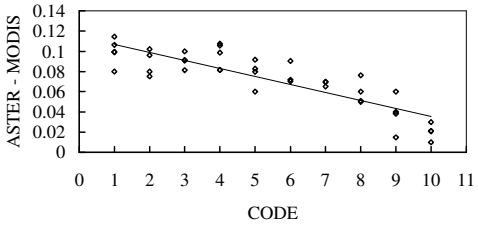

Figure 9. A plot of the differences between ASTER NDVI and MODIS NDVI vs. vegetation fraction codes (AMDI Model).

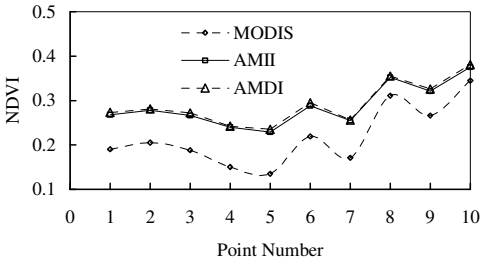

Figure 10. A comparison between predicted NDVI by AMII and AMDI models, and those of MODIS uncorrected values for 10 test samples.

are different from those used for modeling. A summary of the results of this investigation is presented in Table 3.

A comparison between predicted NDVIs through AMII and AMDI models, and MODIS NDVI is presented in Figure 10. The difference between predicted NDVI and observed MODIS NDVI approaches to zero as the amount of vegetation cover increases. Both models are in good agreement with each other while AMDI reading a little lower.

By design, both AMII and AMDI models produce NDVI values higher than those calculated from MODIS. These models were tested using 10 samples where a RMSE of about 0.028 for AMII and 0.018 for AMDI was found. It is found that AMII model can increase the NDVI value up to 87% for pixels containing less than 10% vegetation and 5% for pixels of more than 80% vegetation cover. Increases from AMDI model amount to 84% and 6%, respectively. Figure 10 shows slightly higher readings for the AMII model, particularly for higher vegetation covers.

Since there may also have existed the problem of mixed pixels for ASTER images, then the calculated ASTER NDVIs might have been underestimated and the true value a little higher, so AMII model that reads slightly higher values for NDVI (as shown in Figure 10) is preferred particularly for higher vegetation covers. To promote the ability of these models it is suggested to: (a) evaluate the models for different vegetation covers with precise field and *in situ* assessments, (b) evaluate the models for different atmospheric conditions, (c) investigate the effects of different climates on the models, and (d)

Table 3. The results of evaluation of AMII and AMDI models.

Point no.	MODIS NDVI	ASTER calculated (observed)	Predicted NDVI by AMII	Predicted NDVI by AMDI	Vegetation Cover (%)
1	0.19	0.285	0.268	0.273	57
2	0.205	0.26	0.278	0.281	30
3	0.188	0.251	0.266	0.272	20
4	0.15	0.214	0.24	0.242	20
5	0.135	0.208	0.229	0.235	5
6	0.219	0.261	0.288	0.295	75
7	0.171	0.253	0.255	0.256	25
8	0.311	0.306	0.352	0.355	99
9	0.266	0.284	0.321	0.326	77
10	0.345	0.392	0.375	0.381	80
			RMSE= 0.025	RMSE= 0.028	

[DOR: 20.1001.1.16807073.2009.11.5.7.4]

apply these models to climatological models previously run with unadjusted MODIS NDVI data and compare the results.

REFERENCES

1. Alesheikh, Ali A. and Sadeghi Naeeni Fard, F. 2007. Design and Implementation of a Knowledge Based System to Improve Maximum Likelihood Classification Accuracy. *Can. J. Remote Sens.*, **33(6)**: 459-467.
2. Bolle, H. J. 1996. The Role of Remote Sensing in Understanding and Controlling Land Degradation and Desertification Processes: The EFEDA Research Strategy. *Directorate—General Science, Research and Development, European Commission.* PP. 45–77.
3. Hall, F. G. and Sellers, P. J. 1995. First International Satellite Land Surface Climatology Project (ISLSCP) Field Experiment (FIFE) in 1995. *J. Geophys. Res.*, **100**: 25383- 25396.
4. Hall, F. G., Townshend, J. R. and Engman, E. T. 1995. Status of Remote Sensing Algorithms for Estimation of Land Surface State Parameters. *Remote Sens. Environ*., **51**: 138–156
5. Jiang, Z., Huete, A. R., Chen, J., Chen, Y., Li, J., Yan, G. and Zhang, X. 2006. Analysis of NDVI and Scaled Difference Vegetation Index Retrievals of Vegetation Fraction. *Remote Sens. Environ.,***101**: 366-378
6. Li, J., Lewis, J., Rowland, J., Tappan, G. and Tieszen, L. 2004. Evaluation of Land Performance in Senegal Using Multi-temporal NDVI and Rainfall Series. *J. Arid Environ.*, **59:** 463-480.
7. Malo, A. R. and Nicholson, S. E. 1990. A Study of Rainfall and Vegetation Dynamics in the African Sahel Using Normalized Vegetation Index. *J. Arid Environ.,* **19**:1–24.
8. Milich, L. and Weiss, E. 2000. GAC NDVI Images; Relationship to Rainfall and Potential Evaporation in the Grazing Lands of the Gourma (Northern Sahel) and in the Croplands of Niger–Nigeria Border (Southern Sahel). *Int. J. Remote Sens.,* **21(2):** 261–280.
9. Mobasheri, M. R., Chahardoli, M., Jokar, J. and Farajzadeh, M. 2008. Sugarcane Phenological Date Estimation Using Broad-band Digital Cameras. *Amer. J. Agric. and Biolog. Sci.*, **3(2)**: 468-475.
10. Mobasheri, M. R., Jokar, J., Ziaeian, P. and Chahardoli, M. 2007. On the Methods of Sugarcane Water Stress Detection Using Terra/ASTER Images. *American-Eurasian J. Agric. Environ. Sci*. **2(3)**: 619-627.
11. Reed, B. C., Brown, J. F., Van der Zee, D., Loveland, T. R., Merchant, J. W. and Ohlen, D. 1994. Measuring Phenological Variability from Satellite Imagery. *J. Veget. Sci.,* **5**: 703–714.
12. Sellers, P. J. and Schimel, D. 1993. Remote Sensing of the Land Biosphere and Biogeochemistry in the EOS Era: Science Priorities, Methods and Implementation. *Global and Planetary Change*, **7:** 279- 297.
13. Thiam, A. K. 2003. The Causes and Spatial Pattern of Land Degradation Risk in Southern Mauritania Using Multitemporal AVHRR-NDVI Imagery and Field Data. *Land Degradation and Development,* **14**: 133–142.
14. Townshend, J. R. G., Justice, C. O., Skole, D., Malingreau, J.-P., Cihlar, J., Teillet, P., Sadowski, F. and Ruttenberg, S. 1994. The 1 km Resolution Global Dataset: Needs of the International Geosphere Biosphere Programme. *Int. J.Remote Sens.*, **15**: 3417-3442.

[DOR: 20.1001.1.16807073.2009.11.5.7.4]

بهبود کیفیت شاخص NDVIی بدست آمده از تصاویر MODIS با استفاده از تصاویرASTER

ا. جوادنیا، م. ر. مباشری و غ. ع. کمالی

چکیده

سنجنده‌هایی همچون MODIS و AVHRR از جمله سنجنده‌هایی هستند که با قدرت تفکیک زمانی بالا اطلاعاتی را باتناوب خوب ولی با قدرت تفکیک مکانی پائین جمع‌آوری می‌کنند.. هدف این پژوهش بررسی راهکاریی برای ارتقای شاخص NDVIی بدست آمده از تصاویر MODIS با استفاده از تصاویر ASTER مستقر برروی همان سکو می‌باشد. در این رابطه مقادیر میانگین شاخص بدست آمده از تصاویر ASTER در هر پیکسل مادیس با مقادیر بدست آوده از مادیس مقایسه می‌شوند. در این پژوهش، دو مدل برای اصلاح برآورد شاخص NDVI ارائه شده‌است. در یکی از این دو مدل مستقیماً داده‌های NDVIی بدست آمده از ASTER با NDVIی بدست آمده از MODIS مقایسه شده‌اند (مدل AMII)و در مدل دیگر اختلاف شاخص‌های NDVIی بدست آمده از ASTER و MODIS با کدی که میزان درصد پوشش گیاهی را نشان می‌دهد مقایسه شده‌است (مدل AMDI). دراین رابطه تفاوت بین این دو مقدار شاخص برای پوشش‌های کمتر از ۲۰ درصد، بشتر از ۰/۱ و برای پوشش های بیشتر از ۸۰ درصد در حدود ۰/۰۱ بدست آمد. این نشان می‌دهد که اگر مقادیر اصلاح نشده را در مدلهای اقلیمی برای مناطق نیمه خشک قرار دهیم می‌تواند نتایجی نادرست را بهمراه داشته باشد. هر دو مدل AMII و AMDI مقادیری بالاتر از NDVIی MODIS تولید می‌کنند. این مدلها با استفاده از ۱۰ نمونه مورد آزمایش قرار گرفتند که RMSEیی برابر ۰/۰۲۸ برای AMII و ۰/۰۱۸ برای AMDI بدست آمد. در این رابطه AMII توانست NDVI را تا ۸۷ درصد برای پوشش های کمتر از ۱۰ درصد و ۵ درصد برای پوشش‌های بیشتر از ۸۰ درصد بهبود بخشد. این برای مدل AMDI بترتیب ۸۴ و ۶ درصد بهبود بود.

[DOR: 20.1001.1.16807073.2009.11.5.7.4]